Appl Microbiol Biotechnol (2016) 100:9003–9011
DOI 10.1007/s00253-016-7834-8

MINI-REVIEW

L-Ribose isomerase and mannose-6-phosphate isomerase: properties and applications for L-ribose production

Zheng Xu[1,2] · Yuanyuan Sha[1,2] · Chao Liu[1,2] · Sha Li[1,2] · Jinfeng Liang[1,2] · Jiahai Zhou[3] · Hong Xu[1,2,4]

Received: 22 June 2016 / Revised: 20 August 2016 / Accepted: 23 August 2016 / Published online: 23 September 2016

Abstract L-Ribose is a synthetic L-form monosaccharide. It is a building block of many novel nucleotide analog anti-viral drugs. Bio-production of L-ribose relies on a two-step reaction: (i) conversion of L-arabinose to L-ribulose by the catalytic action of L-arabinose isomerase (L-AI) and (ii) conversion of L-ribulose to L-ribose by the catalytic action of L-ribose isomerase (L-RI, EC 5.3.1.B3) or mannose-6-phosphate isomerase (MPI, EC 5.3.1.8, alternately named as phosphomannose isomerase). Between the two enzymes, L-RI is a rare enzyme that was discovered in 1996 by Professor Izumori's group, whereas MPI is an essential enzyme in metabolic pathways in humans and microorganisms. Recent studies have focused on their potentials for industrial production of L-ribose. This review summarizes the applications of L-RI and MPI for L-ribose production.

Keywords L-Ribose · L-Ribose isomerase · Mannose-6-phosphate isomerase · Hepatitis B virus · L-Sugar

Electronic supplementary material The online version of this article (doi:10.1007/s00253-016-7834-8) contains supplementary material, which is available to authorized users.

✉ Hong Xu
xuh@njtech.edu.cn; xuhonglab@163.com

[1] College of Food Science and Light Industry, Nanjing Tech University, Nanjing, China

[2] State Key Laboratory of Materials-Oriented Chemical Engineering, Nanjing, China

[3] State Key Laboratory of Bio-Organic and Natural Products Chemistry, Shanghai Institute of Organic Chemistry, Chinese Academy of Sciences, Shanghai, China

[4] Jiangsu National Synergetic Innovation Center for Advanced Materials (SICAM), Nanjing, China

Introduction

Sugar isomerases are important enzymes used in the food industry, such as xylose isomerase (EC 5.3.1.5) or, namely, glucose isomerase (GI). GI has great importance in the production of high-fructose corn syrup (HFCS) (Bhosale et al. 1996; Mu et al. 2015). Besides GI, various enzymes have been extensively studied—D-tagatose 3-epimerase (DTE) and D-psicose 3-epimerase (DPE), which catalyze D-psicose synthesis (Itoh et al. 1994; Kim et al. 2006); D-mannose isomerase and D-lyxose isomerase (D-LI), which catalyze D-mannose production; D-ribose-5-phosphate isomerase, D-galactose 6-phosphate isomerase, and L-rhamnose isomerase, which catalyze D-allose synthesis (Menavuvu et al. 2006); and L-arabinose isomerase (L-AI), which catalyzes the synthesis of D-tagatose and L-ribulose (Kim et al. 2004; Oh 2007; Beerens et al. 2012; Mu et al. 2015; Xu et al. 2014). Besides these enzymes, L-ribose isomerase (L-RI) and mannose-6-phosphate isomerase (MPI), which catalyze the conversion of L-ribulose into L-ribose, were recently discovered (Okano 2009; Hu et al. 2011). In 1996, the first L-RI, discovered in *Acinetobacter* sp. strain DL-28, was purified and characterized (Shimonishi and Izumori 1996). In 2001, the gene encoding the enzyme was identified based on the amino acid sequence of the purified native enzyme (Mizanur et al. 2001). Its sequence showed a very low similarity to other known proteins. The highest sequence identities in GenBank were 18 and 19 % to D-LI from *Escherichia coli* strain O157:H7 and *Bacillus subtilis* strain 168, respectively (Yoshida et al. 2014).

2-Deoxy-L-ribose forms the backbone of many anti-viral drugs (e.g., telbivudine, a first-line anti-HBV drug), and it can be chemically synthesized from various monosaccharides such as L-arabinose (through a five-step reaction) and L-ascorbic acid (through an eight-step reaction) (Chong and Chu 2002; Cho et al. 2005). However, the final yields were low,

making these methods low efficient. Using L-ribose as starting material, 2-deoxy-L-ribose can be obtained in a high yield of 60 % (Jung and Xu 1997). Therefore, developing the production of L-ribose will be beneficial for the production of 2-deoxy-L-ribose.

L-Ribose could be obtained by isomerization of L-ribulose using L-RI or MPI; L-ribulose was obtained from L-arabinose using L-AI as a catalyst or from ribitol using washed cells of *Acetobacter aceti* IFO 3281, which yielded a conversion rate of approximately 98 % (Ahmed et al. 1999). Additionally, ribitol was obtained through fermentation by *Trichosporonoides oedocephalis* or *Trichosporonoides megachillensis* using D-glucose as a raw material (Hu et al. 2011; Kawaguchi et al. 2001). However, the yield was low (<30 %) and the cost of extraction of ribitol from the fermentation broth was high. Therefore, it was not economical to produce L-ribose by this process. For the first route, using L-AI, with the addition of borate, L-ribulose was efficiently obtained in a yield of nearly 75 % (Zhang et al. 2009, 2010a, b, 2011). To the best of our knowledge, this is the most efficient route ever reported (Scheme 1). Borate can react with ketose to form L-ribulose-borate complex, resulting in a shift of chemical equilibrium and enhanced the final yields (Zhang et al. 2010a, b). Borate was then eliminated using the method of methanol evaporation (Englesberg 1961). The obtained L-ribulose was used for step (ii) of the reaction to produce L-ribose. In step (ii), isomerization of L-ribulose into L-ribose by L-RI achieved a chemical equilibrium of 30:70 (Ahmed et al. 1999). For isomerization by MPI, the reaction equilibrium was the same to that achieved by L-RI. Thus, both L-RI and MPI were suitable for step (ii) bio-conversion reaction.

In eukaryotes and prokaryotes, MPI catalyzes the conversion of β-D-mannose-6-phosphate (M6P) to D-fructose-6-phosphate (F6P) (Jensen and Reeves 1998). In mammalian cells, MPI was essential for channeling M6P into the glycolytic pathway (Cleasby et al. 1996). MPI has been classified into three types—I, II, and III (Jensen and Reeves 1998; Proudfoot et al. 1994; Sigdel et al. 2015). Type I MPIs are zinc-dependent and homologous mono-functional enzymes, catalyzing a single isomerization reaction (Sigdel et al. 2015; Collins and Hackett 1991; Miles and Guest 1984). Type II MPIs are bi-functional and have limited sequence identity to the type I enzymes, including phosphomannose isomerase-guanosine diphospho-D-mannose pyrophosphorylase (PMI-GMP) from *Pseudomonas aeruginosa* and *Xanthomonas campestris* (Jensen and Reeves 1998). Type III MPIs catalyze reversible isomerization reactions but share little identity with sequences of type I and type II enzymes; this type includes only one enzyme that derived from *Rhizobium meliloti* (Jensen and Reeves 1998; Sigdel et al. 2015). The first crystal structure of MPI was published in Nature Structural Biology journal (Cleasby et al. 1996) as the purpose was to design small molecular inhibitors for this enzyme. Till 2009, professor Oh's group reported that MPI from *B. subtilis* (BsMPI) was identified to have a broad substrate specificity including the ability to convert L-ribulose into L-ribose (Yeom et al. 2009b). Further, developing an "L-ribulose isomerase" has emerged as the new direction in MPI discovery and modification.

The hepatitis virus causes numerous deaths worldwide every year. Development of anti-HBV and anti-HCV drugs is an immediate necessity. A highly efficient technique for manufacturing L-ribose may overcome this problem. To develop a feasible method, enzymatic processing using L-RI and MPI was essential. This review focused on the latest achievements in identification of novel MPI and L-RI and discussed future goals toward L-ribose production using these enzymes.

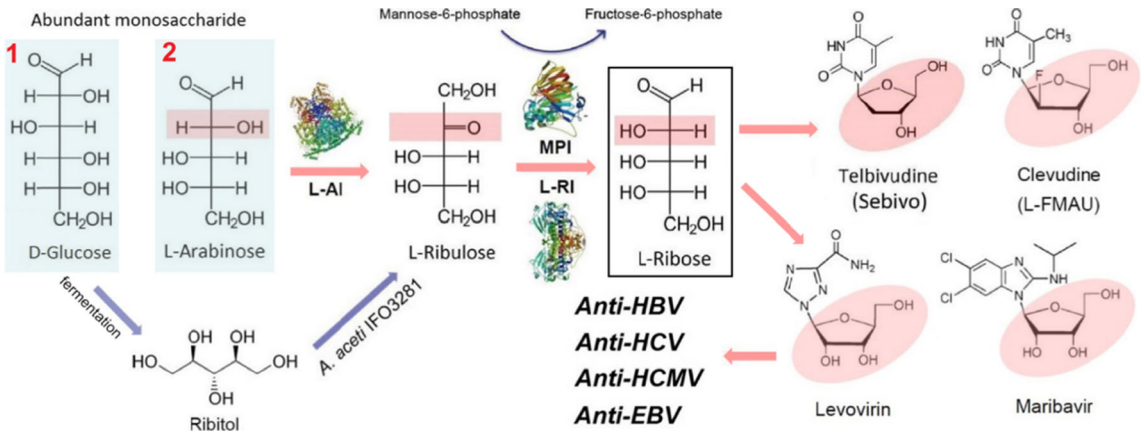

Scheme 1 The two bio-synthetic routes for L-ribose. Route 1 used D-glucose as carbon source to produce ribitol through fermentation by *Trichosporonoides oedocephalis* or *Trichosporonoides megachillensis*. Ribitol was converted into L-ribulose by washed cells of *A. aceti* IFO3281. L-Ribulose was then isomerized into L-ribose by MPI or L-RI. Route 2 used L-arabinose as raw material and L-AI to isomerize it into L-ribulose, which was then converted into L-ribose by L-RI or MPI. L-Ribose and its derivatives are used for the production of many anti-virus drugs

Table 1 Comparison of the enzymatic properties of various L-RIs

Origins	Optimal temp. (°C)	Optimal pH	Stable pH range	M.W. of whole enzyme (kDa)	Sequence identity (%)	Metal ion requirements	References
Acinetobacter sp. DL-28 (native)	30	9.0	7.0–9.0	120 (tetramer)	100	NR	Shimonishi and Izumori 1996
Acinetobacter sp. DL-28 (recombinant)	30	9.0	7.0–9.0	Not reported	100	Mn^{2+}	Mizanur et al. 2001
G. obscurus DSM43160	30–40	9.0	7.0–9.0	120.5 (tetramer)	77.5	No	Hung et al. 2015
C. parahominis MB426	40	9.0	7.0–9.0	Not reported	75.9	No	Morimoto et al. 2013
Actinotalea fermentans	40	8.0	7.5–8.5	Not reported	74.3	No	Xu et al. 2016a, 2016b

Comparison of various L-RIs

The reported L-RIs from different origins were summarized in Table 1. As noted, the optimal temperature of L-RI was in the range of 30–40 °C while the optimal pH was between 7.0 and 9.0. Amino acid sequence analysis revealed a very close identity among reported L-RIs (the lowest was 74.3 % between L-RIs from *Acinetobacter* sp. DL-28 and *Actinotalea fermentans*). Analysis of the effects of metal ions revealed that most L-RIs had no metal requirements because the purified enzyme already contains metals ions and thus had no requirement for exogenous metals ions, except for *Acinetobacter* sp. (AsRI), which needs Mn^{2+} (Mizanur et al. 2001). Ethylene diamine tetraacetic acid (EDTA) showed no influences on the activity of reported L-RI. However, L-RI was reported to be a metalloprotein since all the reported crystal structures have metal ions bound in their active sites. In Table 2, kinetic parameters revealed that L-RI from *Cellulomonas parahominis* MB426 (CpRI) showed the highest catalytic efficiency to form L-ribose. Besides these L-RIs, our group identified L-RI from *A. fermentans*. This enzyme showed optimal temperature and pH of 40 °C and 8.0, respectively, and was tolerant to EDTA and Cu^{2+} (Xu et al. 2016a, b).

L-RI shows broad substrate specificity. In the case of CpRI, effective substrates included L-ribose, L-ribulose, D-lyxose, D-talose, and D-xylulose; the natural substrate was L-ribulose (Morimoto et al. 2013). In the case of L-RI from *Geodermatophilus obscurus* DSM43160 (GoRI), effective substrates were D-lyxose, L-ribose, L-ribulose, and L-sorbose; the natural substrate was L-ribose (Hung et al. 2015). In the case of AsRI, effective substrates were L-ribose and D-lyxose, while the natural substrate was L-ribose (Mizanur et al. 2001). The crystal structure of CpRI and AsRI revealed the presence of Mn^{2+} near the catalytic residues (Terami et al. 2015; Yoshida et al. 2014). It was concluded that L-RI was useful in metabolic pathways using L-ribose as the sole carbon source. Isomerization of L-ribose resulted in the formation of L-ribulose which was then converted to L-ribulose 5-phosphate by L-ribulokinase, and to D-xylulose 5-phosphate by L-ribulose-5-phosphate 4-epimerase, and finally incorporated into the pentose phosphate pathway (Terami et al. 2015).

Stability of L-RI

Stability is one of the most important properties for industrial enzymes. Among the reported L-RI, GoRI was stable at 40 °C for 6 h (Hung et al. 2015) and CpRI was stable at 40 °C for 1 h (Morimoto et al. 2013). When higher than this temperature, it was expected to dissociate from tetrameric to dimeric or monomeric form and become inactive (Terami et al. 2015). However, AsRI was only stable at 30 °C for 10 min

Table 2 Comparison of kinetic parameters of reported L-RIs using different substrates

Origins	Substrate	k_{cat} (min^{-1})	K_m (mM)	$k_{cat}\,K_m^{-1}$ ($mM^{-1}\,min^{-1}$)	V_{max} ($\mu mol\,mg^{-1}\,min^{-1}$)	References
Acinetobacter sp. DL-28	L-Ribose	Not reported	44	Not reported	357	Shimonishi and Izumori 1996 Mizanur et al. 2001
G. obscurus DSM43160	L-Ribose	1224	51.6	21.8	39.2	Hung et al. 2015
C. parahominis MB426	L-Ribose	5710	30.4	188	179	Morimoto et al. 2013
	L-Ribulose	6530	15.4	423	204	
	D-Lyxose	1040	37.1	28.3	32.8	
	D-Talose	947	37.6	25.1	29.6	
	D-Xylulose	1090	32.8	33.3	34.1	

(Shimonishi and Izumori 1996). The *Acidaminococcus fermentans* L-RI (AfRI) has an activity half-life of 7.2 h at 45 °C (Xu et al. 2016a, b). These results implied that stability of L-RI was still not comparable to those of other available industrial enzymes such as GI and L-AI. Protein engineering studies should be carried out in future to improve thermal and pH stability of L-RI. However, there are no reports on stability improvement at this point.

Crystal structure of L-RI

Crystal structures of two L-RIs (AsRI and CpRI) have been revealed (Table 3) (Yoshida et al. 2014; Terami et al. 2015). The overall folding of L-RI adopted a cupin-type β-barrel structure. The catalytic site was between two β-sheets with a bound metal ion. A very flexible loop region was located at the gate for substrate entrance and might involve substrate binding (Yoshida et al. 2014). In the case of these L-RIs, two dimers are associated with each other to form a tetramer (Terami et al. 2015). Moreover, the tetrameric structure of CpRI was essential for its activity and thermal stability (Terami et al. 2015). CpRI was believed to be related to a novel metabolic pathway using L-ribose as the sole carbon source, since expression of it in *E. coli* JM109 made it possible to grow in medium supplemented with L-ribose as the sole carbon source (Terami et al. 2015).

Catalytic mechanism of L-RI

Aldose-ketose isomerase obeys two catalytic mechanisms—cis-enediol intermediate mechanism (Davenport et al. 1991) and hydride-shift mechanism (Whitlow et al. 1991). In a cis-enediol intermediate mechanism, two acid or base catalysts transfer a proton from O2 to O1 and a proton from C2 to C1, respectively. In a hydride-shift mechanism, one acid or base catalyst transfers a proton from O2 to O1 followed by a hydride ion shift between C1 and C2 (van Staalduinen et al. 2010; Manjasetty and Chance 2006). AsRI obeys the rule of cis-enediol intermediate mechanism (Fig. 1), and residues E113/E204 act as acid/base catalysts. Opening of the ring structure of the substrate was enabled by a water molecule coordinated to the metal ion. This water molecule forms hydrogen bonds with O1 and O5 and may help to transfer a proton from O1 to O5 to open the pyranose ring of L-ribose (Yoshida et al. 2014).

Application of L-RI in L-ribose production

The first effective route for L-ribose production was from ribitol to L-ribulose by washed cells of *A. aceti* IFO 3281, and then L-ribulose was converted into L-ribose by L-RI (Ahmed et al. 1999). However, as an alternative pathway, L-ribose could be obtained by using L-arabinose as a raw material and by the use of another aldose-ketose isomerase, namely, L-AI. L-AI isomerizes L-arabinose into L-ribulose. However, the equilibrium ratio for this reaction was 90:10, demonstrating a poor yield for L-ribulose. Nevertheless, high yield of L-ribulose could be obtained with the addition of boric acid in alkaline conditions, as previously reported (Zhang et al. 2010a, b). Meanwhile, by the use of novel immobilization technique for L-AI, L-ribulose yield increased to 62 % (Xu et al. 2016a, b). Hung et al. used L-AI from *Thermoanaerobacterium saccharolyticum* strain NTOU1 and recombinant GoRI to produce L-ribose from L-arabinose, and the highest conversion rate was 15.9 % (Hung et al. 2015). AsRI was expressed in L-ribulokinase-deficient *E. coli* UP1110 and *Lactobacillus plantarum* BPT197 strains, and the resting cells achieved a highest conversion rate of 20 % from L-arabinose (Helanto et al. 2009). A problem that needed immediate attention was the separation of L-ribose from the final reaction solution. Simulated moving bed chromatography (SMBC) would be a promising technique as several successful separations using this approach have been reported, including purification of D-fructose from high-fructose corn syrup and amino acid separation (Juza et al. 2000).

Table 3 Released structural information of L-RI in the PDB database

Origins	PDB ID	Description	Resolution (Å)	Sequence identity (%)	References
Acinetobacter sp. DL-28	4Q0P	AsRI and L-ribose	1.93	100	Yoshida et al. 2014
	4Q0Q	AsRI and L-ribulose	1.93		
	4Q0S	AsRI and L-ribitol	1.93		
	4Q0U	E204Q mutant and L-ribose	1.98		
	4Q0V	E204Q mutant and L-ribulose	1.98		
Cellulomonas parahominis	3WW3	*apo*	1.90	75.9	Terami et al. 2015
	3WW1	CpRI and L-ribose	1.95		
	3WW4	CpRI and L-allose	1.95		
	3WW2	CpRI and L-psicose	2.00		

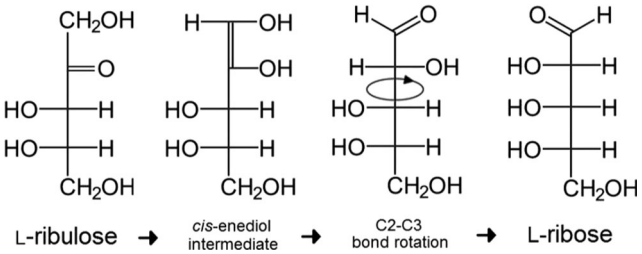

Fig. 1 Catalytic mechanism of isomerization from L-ribulose to L-ribose by L-RI

Comparison of different MPI

Till now, MPI isolated from eight origins have been reported including those from *Homo sapiens* (Proudfoot et al. 1994), *Thermus thermophilus* (Yeom et al. 2011b), *Thermotoga neapolitana* (Shin et al. 2013), *Bacillus subtilis* (Yeom et al. 2009b), *Candida albicans* (Proudfoot et al. 1994), *Saccharomyces cerevisiae* (Wells et al. 1993), *Salmonella typhimurium* (Sagurthi et al. 2009), *Geobacillus thermodenitrificans* (Yeom et al. 2009a), and *Bacillus amyloliquefaciens* (Sigdel et al. 2015). Among these, three origins were reported to be able to produce L-ribose, including *T. thermophilus*, *G. thermodenitrificans*, and *B. subtilis*. The reported MPIs were compared, and their properties are summarized in Table 4. Sequence similarities among these MPI were rather low. Interestingly, as shown in GenBank, several MPIs were reported to exist in the same bacteria (*B. subtilis* str. 168) as isoenzymes (Table S1). One should notice that the k_{cat} values of MPI were much higher than those of L-RI.

Site-directed mutagenesis of MPI

Among the reported MPI, the one from *G. thermodenitrificans* (GtMPI) and *T. thermophilus* (TtMPI) were subjected to site-directed mutagenesis. The essential residues affecting enzyme activity were summarized in Table 5. The mutant R142N of TtMPI showed better catalytic properties than the wild-type enzyme (Yeom et al. 2011a, b). In the case of TtMPI, four residues (H50, E67, H122, and E132) were responsible for metal ion binding, and their alanine mutants lost activities. The other five residues (R11, K37, Q48, K65, and R142) were responsible for substrate binding. The aromatic ring of residue W13 was essential for enzyme activity. Residues W17, N90, and L129 were important for the activity of GtMPI. Among these mutants, the triple-site mutant W17Q/N90A/L129F showed the highest k_{cat} and catalytic efficiency (112,098 s^{-1} and 1120 s^{-1} mM^{-1}, respectively) (Lim et al. 2012). The BsMPI (GenBank accession no. AF324506) was mutated into an "L-ribose isomerase" (lost original activity for mannose-6-

Table 4 Comparison of enzymatic properties and kinetic parameters of reported MPI

Origins	Optimal temperature	Optimal pH	K_m[a] (mM)	k_{cat} K_m^{-1}[a] (mM^{-1} s^{-1})	K_m[b] (mM)	k_{cat} K_m^{-1}[b] (mM^{-1} s^{-1})	References
G. thermodenitrificans	70 °C	7.0	NR	NR	149/470[c]	158/61[c]	Yeom et al. 2009a; Lim et al. 2012
G. thermodenitrificans[d] mutant	70 °C	7.0	NR	NR	100	1120	Lim et al. 2012
T. thermophilus	80 °C[a]/75 °C[b]	7.0	0.21	6685	136	374	Yeom et al. 2011a
T. thermophilus[e] mutant	NR	NR	NR	NR	140	579	Yeom et al. 2011b
B. subtilis	40 °C	7.5	29	770	849/998[c]	43.5/17.6[c]	Yeom et al. 2009b
B. subtilis mutant[f]	NR	NR	0	0	569[c]	45.9[c]	Yeom et al. 2013
B. amyloliquefaciens	70 °C	7.5	7.6	13,900	NR	NR	Sigdel et al. 2015
Homo sapiens	37 °C	8.0	0.25	337	NR	NR	Proudfoot et al. 1994
Candida albicans	37 °C	8.5	1.24	774	NR	NR	Proudfoot et al. 1994
Saccharomyces cerevisiae	37 °C	8.0	0.65	1206	NR	NR	Wells et al. 1993
Salmonella typhimurium	37 °C	8.5	1.34	435	NR	NR	Collins and Hackett 1991 Sagurthi et al. 2009
E. coli	NR	NR	NR	NR	NR	NR	Miles and Guest 1984

NR not reported

[a] The substrate was mannose-6-phosphate

[b] The substrate was L-ribulose

[c] The substrate was L-ribose

[d] Mutant W17Q/N90A/L129F

[e] Mutant R142N

[f] Mutant R192N

Table 5 Site directed mutants of reported MPI

Origins	Mutants	Enzyme activity (U/mg)	k_{cat} (s^{-1})	k_{cat} K_m^{-1} (mM^{-1} s^{-1})	References
T. thermophilus	WT	1493	50,644	374	Yeom et al. 2011a
	R142N	2152	81,063	579	Yeom et al. 2011b
G. thermodenitrificans	WT	NR	23,546	158	Lim et al. 2012
	L129F	NR	55,123	227	
	N90A/L129F	NR	85,715	965	
	W17Q/N90A/L129F	NR	112,098	1120	

The substrate for kinetic parameters determination was L-ribulose

phosphate) by site-directed mutagenesis of R192A. Moreover, its counterpart R192N showed 3.5-fold enhanced activity for formation of L-ribose (Yeom et al. 2013).

Stability of MPI

GtMPI showed half-lives of 338, 73, 27, 17, and 6 h at 60, 65, 70, 75, and 80 °C, respectively (Yeom et al. 2009a). The GtMPI mutants L129F, N90A/L129F, and W17Q/N90A/L129F were stable at 60–65 °C for 12 h and retained 13, 26, and 32 % of activity at 80 °C, respectively (Lim et al. 2012). This implied that such mutations enhanced thermostability of the enzyme. Thermostability of the immobilized *E. coli* whole cell expressing GtAI and GtMPI was also evaluated, and half-lives at 55, 60, 65, and 70 °C were 50, 36, 29, and 13 h, respectively. The immobilized cells expressing GtAI and GtMPI mutant (W17Q/N90A/L129F) showed 4–29-fold enhanced thermostability at 55–70 °C (Kim et al. 2014).

Crystal structure of MPI

MPI is essential for the biosynthesis of fungal cell wall. Absence of MPI activity in yeasts caused cell lysis; thus, this enzyme is a potential target for inhibition of fungal infection and might be used as anti-fungal drug. The first studied structure of MPI was of the one derived from *C. albicans* (Cleasby et al. 1996). Crystal structures of MPI from six origins (ten structures in total) have been deposited into the PDB database (Table 6). Among them, two origins, namely *Salmonella typhimurium* and *Pyrobaculum aerophilum*, included both *apo* and *holo* structures. The 1.8-Å crystal structure of BsMPI was released in the PDB database (accession no. 1QWR, doi 10.2210/pdb1qwr/pdb) as part of the structural genomics initiative, and no corresponding paper was published. One should notice that this BsMPI was not the one reported by Yeom et al., whose GenBank accession number was AF324506 (2009b; 2013). Similar to BsMPI, no related paper was published for MPI from *Archaeoglobus fulgidus* and *Helicobacter pylori*. The structure of *T. thermophilus* was modeled using the crystal structure of BsMPI as template. It was observed that four residues H50, E67, H122, and E132 were metal-binding residues and five residues R11, K37, Q48, K65, and R142 were substrate-binding residues. Moreover, W13 might be related to the function of sealing off the active site (Yoem 2011a).

Catalytic mechanism of MPI

The catalytic mechanism of MPI was believed to be the *cis*-enediol mechanism (Sagurthi et al. 2009). Type I MPI from *C. albicans*, as well as the one from *P. aerophilum*, was identified to obey the *cis*-enediol mechanism according to the *apo* and *holo* crystal structures (Cleasby et al. 1996; Swan et al. 2004). Arginine 304 was proved to be the active site residue of MPI from *C. albicans* (Wells et al. 1994), while its function was further confirmed by crystal structure (Cleasby et al. 1996). The enzyme activity of MPI from *S. cerevisiae* was zinc-dependent. It was also reported to be inhibited by zinc ion (Wells et al. 1993).

Applications of MPI in L-ribose production

An enzymatic process was reported using purified L-AI and MPI enzymes (both derived from *G. thermodenitrificans*) to produce L-ribose. Using 500 g/L L-arabinose as substrate and 8 U/mL L-AI and 20 U/mL MPI (AI/MPI ratio, 1:2.5) as biocatalysts, this method achieved a whole conversion yield of 23.6 % and a volumetric productivity of 39.3 g/L·h (Yeom 2009c). Using 300 g/L L-ribulose as substrate and 2 mg/mL enzyme, the wild-type TtMPI resulted in a conversion rate of 70 % and a volumetric productivity of 71 g/L h^{-1} in 3 h. Under similar conditions, its mutant R142N showed higher volumetric productivity of 107 g/L h^{-1} (Yeom et al. 2011b). By using alginate-immobilized *E. coli* whole cell

Table 6 Released structural information of MPI in PDB database

Origins	PDB ID	Description	Resolution (Å)	Sequence identity (%)	References
Salmonella typhimurium	2WFP	St-MPI-EDO	1.67	100	Gowda et al. 2008
	3H1Y	St-MPI-F6P-Zn^{2+}	2.04		
	3H1W	St-MPI-Zn^{2+}-Y^{3+}	1.94		Sagurthi et al. 2009
	3H1M	St-MPI-Zn^{2+}	2.5		
Candida albicans	1PMI	*apo*	1.7	27.0	Tolley et al. 1994
					Cleasby et al. 1996
Archaeoglobus fulgidus	1ZX5	*apo*	2.3	14.7	Not published
Bacillus subtilis	1QWR	*apo*	1.8	15.2	Not published
Helicobacter pylori	2QH5	*apo*	2.3	9.6	Not published
Pyrobaculum aerophilum	1TZB	*apo*	1.16	14.4	Swan et al. 2004
	1TZC	Pa-MPI-5-phosphoarabinonate	1.45		

co-expressing L-AI and MPI, it was feasible to obtain 99 g/L L-ribose in a conversion yield of 33 % (*w*/*w*) and productivity of 33 g/L h^{-1} using 300 g/L L-arabinose as substrate, whereas immobilized cells contained 13 U/mL L-AI and 50 U/mL MPI mutant (W17Q/N90A/L129F) (Kim et al. 2014).

Problems and further goals

The current problem for the production of L-RI was lacking enzyme source. In GenBank, bacteria from only five origins contain proteins being annotated as L-ribose isomerase. This implied that L-RI was rarely found in microorganisms. To screen more L-RI-producing microorganisms, studies should be focused on bacteria with an ability to utilize L-ribose as the sole carbon source. Currently available L-RI showed problems such as lower k_{cat} value than that of MPI, as well as poor thermal stability. L-ribulose was reported to be unstable in alkaline or thermal conditions (De Muynck et al. 2006). However, the optimal pH of L-RI reaction was alkaline from 7.0 to 9.0, which is harmful to substrate. Directed evolution and site-directed mutation should be carried out to improve these properties. Moreover, feasible methods should be established including usage of novel materials for enzyme or cell immobilization. Until now, no site-directed mutation was available for L-RI. Further attempts need to be done on L-RI modification to enhance its stability, to fulfill the industrial requirements. One problem of MPI might be the high reaction temperature, 70–75 °C for GtMPI and TtMPI. This might cause degradation of L-ribulose during reaction. It is hard to modify current MPI by rational design due to the lack of structural information. Crystal structures of the potential industrial candidates of MPI need to be revealed.

Compliance with ethical standards

Ethical approval This article does not contain any studies with human participants performed by any of the authors.

Funding We gratefully acknowledge the financial support from the National Natural Science Foundation of China (no. 31400053 to Z. Xu), the Natural Science Foundation of Jiangsu Province (no. BK20140933 to Z. Xu), the Jiangsu Province Science and Technology Support Plan Project (no. BE2015366 to H. Xu), the Science and Technology Program of Joint Innovation Fund—A Prospective Joint Research Project in Jiangsu Province (no. BY2014005-10 to J.F. Liang), and the State Key Laboratory of Materials-Oriented Chemical Engineering (no. KL15-09 to J. Zhou).

Conflict of interest The authors declare that there is no conflict of interest.

References

Ahmed Z, Shimonishi T, Bhuiyan SH, Utamura M, Takada G, Izumori K (1999) Biochemical preparation of L-ribose and L-arabinose from ribitol: a new approach. J Biosci Bioeng 88(4):444–448

Beerens K, Desmet T, Soetaert W (2012) Enzymes for the biocatalytic production of rare sugars. J Ind Microbiol Biot 39(6):823–834

Bhosale SH, Rao MB, Deshpande VV (1996) Molecular and industrial aspects of glucose isomerase. Microbiol Rev 60(2):280–300

Cho BH, Kim JH, Jeon HB, Kim KS (2005) A new efficient and practical synthesis of 2-deoxy-L-ribose. Tetrahedron 61(18):4341–4346

Chong Y, Chu CK (2002) Efficient synthesis of 2-deoxy-L-erythro-pentose (2-deoxy-L-ribose) from L-arabinose. Carbohyd Res 337(5):397–402

Cleasby A, Wonacott A, Skarzynski T, Hubbard RE, Davies GJ, Proudfoot AE, Bernard AR, Payton MA, Wells TN (1996) The X-ray crystal structure of phosphomannose isomerase from *Candida albicans* at 1.7 Å resolution. Nat Struct Mol Biol 3(5):470–479

Collins LV, Hackett J (1991) Sequence of the phosphomannose isomerase-encoding gene of *Salmonella typhimurium*. Gene 103(1):135–136

Davenport RC, Bash PA, Seaton BA, Karplus M, Petsko GA, Ringe D (1991) Structure of the triosephosphate isomerase-phosphoglycolohydroxamate complex: an analog of the intermediate on the reaction pathway. Biochemistry 30(24):5821–5826

De Muynck C, Pereira C, Soetaert W, Vandamme E (2006) Dehydrogenation of ribitol with *Gluconobacter oxydans*: production and stability of L-ribulose. J Biotechnol 125(3):408–415

Englesberg E (1961) Enzymatic characterization of 17 L-arabinose negative mutants of *Escherichia coli*. J Bacteriol 81(6)

Gowda G, Sagurthi SR, Savithri HS, Murthy MRN (2008) Cloning, expression, purification, crystallization and preliminary X-ray crystallographic analysis of the mannose 6-phosphate isomerase from *Salmonella typhimurium*. Acta Crystallogr Sect F Struct Biol Cryst Commun 64(2):81–84

Helanto M, Kiviharju K, Granström T, Leisola M, Nyyssölä A (2009) Biotechnological production of L-ribose from L-arabinose. Appl Microbiol Biotechnol 83(1):77–83

Hu C, Li L, Zheng Y, Rui L, Hu C (2011) Perspectives of biotechnological production of L-ribose and its purification. Appl Microbiol Biotechnol 92(3):449–455

Hung XG, Yu MY, Chen YC, Fang TY (2015) Characterization of a recombinant L-ribose isomerase from *Geodermatophilus Obscurus* DSM 43160 and application of this enzyme to the production of L-ribose from L-arabinose. J Mar Sci Tech Taiw 23(4):558–566

Itoh H, Okaya H, Khan AR, Tajima S, Hayakawa S, Izumori K (1994) Purification and characterization of D-tagatose 3-epimerase from Pseudomonas sp. ST-24. Biosci Biotechnol Biochem 58(12): 2168–2171

Jensen SO, Reeves PR (1998) Domain organisation in phosphomannose isomerases (types I and II). Biochim Biophys Acta Protein Struct Mol Enzymol 1382(1):5–7

Jung ME, Xu Y (1997) Efficient syntheses of L-ribose and 2-deoxy L-ribose from D-ribose and L-arabinose. Tetrahedron Lett 38(24): 4199–4202

Juza M, Mazzotti M, Morbidelli M (2000) Simulated moving-bed chromatography and its application to chirotechnology. Trends Biotechnol 18(3):108–118

Kawaguchi T, Hara M, Ueda M (2001) Process for producing L-ribose. EP1083234

Kim P (2004) Current studies on biological tagatose production using L-arabinose isomerase: a review and future perspective. Appl Microbiol Biotechnol 65(3):243–249

Kim HJ, Hyun EK, Kim YS, Lee YJ, DK O (2006) Characterization of an *Agrobacterium tumefaciens* D-psicose 3-epimerase that converts D-fructose to D-psicose. Appl Environ Microb 72(2):981–985

Kim KR, Seo ES, Oh DK (2014) L-Ribose production from L-arabinose by immobilized recombinant *Escherichia coli* co-expressing the L-arabinose isomerase and mannose-6-phosphate isomerase genes from *Geobacillus thermodenitrificans*. Appl Microbiol Biotechnol 172(1):275–288

Lim YR, Yeom SJ, DK O (2012) Production of L-ribose from L-ribulose by a triple-site variant of mannose-6-phosphate isomerase from *Geobacillus thermodenitrificans*. Appl Environ Microb 78(11): 3880–3884

Manjasetty BA, Chance MR (2006) Crystal structure of *Escherichia coli* L-arabinose isomerase (ECAI), the putative target of biological tagatose production. J Mol Biol 360(2):297–309

Menavuvu BT, Poonperm W, Leang K, Noguchi N, Okada H, Morimoto K, Granström TB, Takada G, Izumori K (2006) Efficient biosynthesis of D-allose from D-psicose by cross-linked recombinant L-rhamnose isomerase: separation of product by ethanol crystallization. J Biosci Bioeng 101(4):340–345

Miles JS, Guest JR (1984) Complete nucleotide sequence of the fumarase gene fumA, of *Escherichia coli*. Nucleic Acids Res 12(8):3631–3642

Mizanur RM, Takata G, Izumori K (2001) Cloning and characterization of a novel gene encoding L-ribose isomerase from *Acinetobacter* sp. strain DL-28 in *Escherichia coli*. Biochim Biophys Acta (BBA) Gene Struct Expr 1521(1):141–145

Morimoto K, Terami Y, Maeda YI, Yoshihara A, Takata G, Izumori K (2013) Cloning and characterization of the L-ribose isomerase gene from *Cellulomonas parahominis* MB426. J Biosci Bioeng 115(4): 377–381

Mu W, Yu L, Zhang W, Zhang T, Jiang B (2015) Isomerases for biotransformation of D-hexoses. Appl Microbiol Biotechnol 99(16):6571–6584

Oh DK (2007) Tagatose: properties, applications, and biotechnological processes. Appl Microbiol Biotechnol 76(1):1–8

Okano K (2009) Synthesis and pharmaceutical application of L-ribose. Tetrahedron 65(10):1937–1949

Proudfoot AE, Turcatti G, Wells TN, Payton MA, Smith DJ (1994) Purification cDNA cloning and heterologous expression of human phosphomannose isomerase. Eur J Biochem 219(1–2):415–423

Sagurthi SR, Gowda G, Savithri HS, Murthy MRN (2009) Structures of mannose-6-phosphate isomerase from *Salmonella typhimurium* bound to metal atoms and substrate: implications for catalytic mechanism. Acta Crystallogr Sec D Biol Crystallogr 65(7):724–732

Shimonishi T, Izumori K (1996) A new enzyme, L-ribose isomerase from *Acinetobacter* sp. strain DL-28. J Ferment Bioeng 81(6):493–497

Shin HC, Jang MU, Lee HG, Kim MJ, Park JM, Jang KI, Kim TJ (2013) Effect of temperature and pH on interconversion between fructose and mannose catalyzed by *Thermotoga neapolitana* mannose-6-phosphate isomerase. Food Sci Biotechnol 22(1):39–44

Sigdel S, Singh R, Kim TS, Li J, Kim SY, Kim IW, Jung WS, Pan CH, Kang YC, Lee JK (2015) Characterization of a mannose-6-phosphate isomerase from *Bacillus amyloliquefaciens* and its application in fructose-6-phosphate production. PLoS One 10(7): e0131585

Swan MK, Hansen T, Schönheit P, Davies C (2004) A novel phosphoglucose isomerase (PGI)/phosphomannose isomerase from the crenarchaeon *Pyrobaculum aerophilum* is a member of the PGI superfamily structural evidence at 1.16 Å resolution. J Biol Chem 279(38):39838–39845

Terami Y, Yoshida H, Uechi K, Morimoto K, Takata G, Kamitori S (2015) Essentiality of tetramer formation of *Cellulomonas parahominis* L-ribose isomerase involved in novel L-ribose metabolic pathway. Appl Microbiol Biotechnol 99(15):6303–6313

Tolley S, Davies G, Hubbard RE, Smith DJ, Proudfoot AE, Payton MA, Cleasby A, Wonacott A, Wells TN (1994) Crystallization and preliminary X-ray analysis of *Candida albicans* phosphomannose isomerase. J Mol Biol 237(3):349–350

van Staalduinen LM, Park CS, Yeom SJ, Adams-Cioaba MA, Oh DK, Jia Z (2010) Structure-based annotation of a novel sugar isomerase from the pathogenic *E. coli* O157:H7. J Mol Biol 401(5):866–881

Wells TN, Coulin F, Payton MA, Proudfoot AE (1993) Phosphomannose isomerase from *Saccharomyces cerevisiae* contains two inhibitory metal ion binding sites. Biochemistry 32(5):1294–1301

Wells TN, Scully P, Magnenat E (1994) Arginine 304 is an active site residue in phosphomannose isomerase from *Candida albicans*. Biochemistry 33(19):5777–5782

Whitlow M, Howard AJ, Finzel BC, Poulos TL, Winborne E, Gilliland GL (1991) A metal-mediated hydride shift mechanism for xylose isomerase based on the 1.6 Å *Streptomycs rubiginosus* structure with xylitol and D-xylose. Proteins Struct Function Bioinformatics 9(3):153–173

Xu Z, Li S, Feng X, Liang J, Xu H (2014) L-Arabinose isomerase and its use for biotechnological production of rare sugars. Appl Microbiol Biotechnol 98(21):8869–8878

Xu H, Liu C, Xu Z, Wang X, Li S, Feng XH (2016a) An L-ribose isomerase and its application in bio-production of L-ribose. Chinese patent no. 201610218779.3

Xu Z, Wang R, Liu C, Chi B, Gao J, Chen B, Xu H (2016b) A new L-arabinose isomerase with copper ion tolerance is suitable for creating protein-inorganic hybrid nanoflowers with enhanced enzyme activity and stability. RSC Adv 6:30791–30794

Yeom SJ, Kim NH, Yoon RY, Kwon HJ, Park CS, Oh DK (2009a) Characterization of a mannose-6-phosphate isomerase from *Geobacillus thermodenitrificans* that converts monosaccharides. Biotechnol Lett 31(8):1273–1278

Yeom SJ, Ji JH, Kim NH, Park CS, Oh DK (2009b) Substrate specificity of a mannose-6-phosphate isomerase from *Bacillus subtilis* and its application in the production of L-ribose. Appl Environ Microb 75(14):4705–4710

Yeom SJ, Kim NH, Park CS, Oh DK (2009c) L-Ribose production from L-arabinose by using purified L-arabinose isomerase and mannose-6-phosphate isomerase from *Geobacillus thermodenitrificans*. Appl Environ Microb 75(21):6941–6943

Yeom SJ, Kim YS, Lim YR, Jeong KW, Lee JY, Kim Y, Oh DK (2011a) Molecular characterization of a novel thermostable mannose-6-phosphate isomerase from *Thermus thermophilus*. Biochimie 93(10):1659–1667

Yeom SJ, Seo ES, Kim BN, Kim YS, Oh DK (2011b) Characterization of a mannose-6-phosphate isomerase from *Thermus thermophilus* and increased L-ribose production by its R142N mutant. Appl Environ Microb 77(3):762–767

Yeom SJ, Kim YS, Oh DK (2013) Development of novel sugar isomerases by optimization of active sites in phosphosugar isomerases for monosaccharides. Appl Environ Microb 79(3):982–988

Yoshida H, Yoshihara A, Teraoka M, Terami Y, Takata G, Izumori K, Kamitori S (2014) X-ray structure of a novel L-ribose isomerase acting on a non-natural sugar L-ribose as its ideal substrate. FEBS J 281(14):3150–3164

Zhang YW, Prabhu P, Lee JK (2009) Immobilization of Bacillus licheniformis L-arabinose isomerase for semi-continuous L-ribulose production. Biosci Biotech Biochem 73(10):2234–2239

Zhang YW, Prabhu P, Lee JK (2010a) Alginate immobilization of recombinant *Escherichia coli* whole cells harboring L-arabinose isomerase for L-ribulose production. Bioprocess Biosyst Eng 33(6):741–748

Zhang YW, Jeya M, Lee JK (2010b) L-Ribulose production by an *Escherichia coli* harboring L-arabinose isomerase from *Bacillus licheniformis*. Appl Microbiol Biotechnol 87(6):1993–1999

Zhang YW, Jeya M, Lee JK (2011) Enhanced activity and stability of L-arabinose isomerase by immobilization on aminopropyl glass. Appl Microbiol Biotechnol 89(5):1435–1442